Advanced Powder Technology 34 (2023) 104259

Contents lists available at ScienceDirect

Advanced Powder Technology

journal homepage: www.elsevier.com/locate/apt

Rapid Communication

Modelling and estimating the Blaine number of iron ore concentrate by response surface methodology and Monte Carlo simulation

Seyed Hadi Shahcheraghi [a,*], Mehdi Dianatpour [b], Mohammad Hayati [c]

[a] Department of Research, Innovation and Localization, Gohar Zamin Iron Ore Company, Sirjan, Kerman, Iran
[b] Department of Laboratory & Quality Control, Gohar Zamin Iron Ore Company, Sirjan, Kerman, Iran
[c] Department of Mining Engineering, Faculty of Engineering, Lorestan University, Khorramabad, Iran

ARTICLE INFO

Article history:
Received 26 July 2023
Received in revised form 14 October 2023
Accepted 18 October 2023

Keywords:
Blaine number
Particles physical properties
Response Surface method
Reliability analysis
Iron ore concentrate

ABSTRACT

The Blaine number of iron ore concentrate is a key parameter in the iron and steel chain, especially pelletizing. In this study, a novel and comprehensive strategy was introduced for modelling and estimating the Blaine number of iron ore concentrate by using the particles physical properties (particles size distribution and shape)-based Response Surface method and Monte Carlo simulation. The proposed strategy was implemented for modelling the Blaine number of concentrate produced in an industrial iron ore processing plant. Then, the obtained model was validated by using industrial data. The results showed that the proposed strategy and obtained model can be used as a powerful technique for modelling and relatively accurate predicting the Blaine number of iron ore concentrate produced in industrial plants and a suitable alternative to the conventional measurement methods.

1. Introduction

The Blaine number of iron ore concentrate is one of the most important parameters for controlling the pelletizing process in the iron and steel industry [1–4]. The specific surface area (SSA) of powder materials or Blaine number is defined as quotient of the available surface inclusive of all open inner surfaces divided by the mass ($cm^2\ g^{-1}$), and measured based on the air permeability of a packed bed of particles [5,6].

The lower and the higher Blaine number refers to the coarser and the finer size of concentrate particles, respectively. The iron ore concentrate with the higher Blaine number causes problem in pellets making [1,2]. Moreover, it requires the higher grinding energy during preparation to achieve the required Blaine fineness [7]. The iron ore concentrate with the lower Blaine number doesn't provide the sufficient strength both to the green and indurated pellets [8]. Therefore, the relatively accurate prediction of Blaine number in the shortest possible time is necessary to control and optimize the production process of iron ore concentrate with desired Blaine number and consequently, pellets with required quality. Accordingly, it is necessary to find a mathematical model that can predict the Blaine number in the shortest possible time. However, this depends on the simplicity and the measurement duration of model's parameters [9]. Although there are many researches about the effect of Blaine number on the pelleting process and the pellets quality [1,2,8,10–12], few researches have investigated the effect of different parameters on the Blaine number of iron ore concentrate.

Abazarpoor et al. (2018) studied the effect of high-pressure grinding rolls (HPGR) operational parameters including the feed moisture, the specific pressure and the roll speed on the dimensional properties of pellet feed using factorial methodology. They found that increasing the specific pressure and decreasing the roll speed would increase the Blaine number. Moreover, according to their findings, the feed moisture of HPGR had the least effect on the Blain number [13]. Accordingly, it can be concluded that the specific pressure and the roll speed parameters affect two physical characteristics of particles, i.e., the particles size distribution and the shape. In the other words, the particle size distribution and the shape control the Blaine number.

Hosseini Nasab and Sadeghi (2020) investigated the effect of the particles size distribution and the mineral type on the Blaine number of iron ore concentrate. They found that increasing the percentage of particles finer than 45 μm resulted in higher Blaine numbers. Moreover, the presence of clay minerals in the iron ore concentrate led to an increase in the Blaine number [14]. Accordingly, it can be concluded that the presence of clay minerals led

* Corresponding author. Tel.: +98–913–2531004
E-mail addresses: h.shahcheraghi@goharzamin.com, shahcheraghi66@gmail.com (S.H. Shahcheraghi).

https://doi.org/10.1016/j.apt.2023.104259

to change of the Blaine number due to their size distribution and shape. In other words, clay minerals are often characterized by their small size, plate-like shape (e.g., Kaolinite), and large specific surface, which their small size can explain their high Blaine number [14].

Therefore, two particles physical properties including the particles size distribution and the shape are the most important parameters controlling the Blaine number of iron ore concentrate. Zhang and Napier-Munn (1995) proposed a model based on particle size distribution to predict the surface area of spherical particles. Applications of this model have showed good description of Blaine number of particles with regular geometric shapes [15].

Generally, there are three ways of experimental determining the Blaine number: the international standard of ISO 21283 [16], the ASTM C204-16 [17], and the volumetric static multi-point method known as the BET (Brunauer–Emmett–Teller) method [18]. Currently, the most common method of determining the Blaine number of iron ore concentrate in the laboratory of iron ore mines is ISO 21283 by Blaine meter. The experimental methods of determining the Blaine number have fundamental limitations, and the existence of a mathematical model to replace the experimental methods is very necessary. The most important limitations are as following:

- A large number of daily samples to determine the Blaine number;
- The long time required for the determination of Blaine number from sample preparation to Blaine test [16];
- The presence of human and systematic errors;
- High consumption of expensive CRM (Certified Reference Material) per month due to daily calibration of the Blaine meter: according to our experience and observation in the laboratory, it's noticeable that CRM can only be used once and if it is used again, the Blaine number decreases and it lacks accuracy and validity; According to our observation, the possible reason for this is that the fine particles of CRM stick to the mouth of the funnel after each use and as a result, by removing the fine particles, the Blaine number of the used CRM is reduced.
- The sensitivity of the Blaine meter to the environmental conditions such as moisture and temperature [16].

According to some research [10,13–15,19,20], the well-known models, due to simplification, are only applicable for predicting the Blaine number of particles with the regular geometric shapes. In this study, with the aim of removing the mentioned limitations, a comprehensive strategy for modeling and predicting the Blaine number of iron ore concentrate depending on the physical nature of the particles by Response Surface methodology (RSM) and Monte Carlo simulation has been proposed. The RSM was used as a powerful statistical method for finding the most suitable functional relationship, especially non-linear, between the independent variables (i.e., the parameters controlling the Blaine number of iron ore concentrate in each particle size fraction) affecting the Blaine number. The Monte Carlo simulation was used for the sensitivity and reliability analysis of the final model. The obtained model has been validated with samples and data collected from iron ore processing in Gohar Zamin Iron Ore Company, Gol-e-Gohar Mining & Industrial Company, and Chadormalu Mining and Industrial Company. It's noticeable that the production process of iron ore concentrate is similar in all three companies in order to ensure: (1) the same conditions of data production, and (2) the possibility of directly using the results of the final model presented in the factories with similar processes (no need to calibrate the model). For example, the type and number of grinding steps affect the Blaine number [21].

2. Materials and methods

2.1. Process description of iron ore processing plant

The iron ore processing plant of Gohar Zamin Iron Ore Company, which is located in the Gol-e-Gohar mine No. 3 (Sirjan–Iran), consists of five units (Fig. 1): (1) the primary crushing unit consists of a Gyratory crusher to reduce the particles size to less than 300 mm; (2) the secondary crushing unit consists of several cone crushers to reduce the particles size to less than 50 mm; (3) the grinding unit consists of a high-pressure grinding roll (HPGR) and a ball mill to produce the product with d_{80} less than 115 μm; (4) the magnetic separation unit consists of cobber, roughers and cleaners; and (5) the dewatering unit to produce the iron ore concentrate with a moisture less than 8 %.

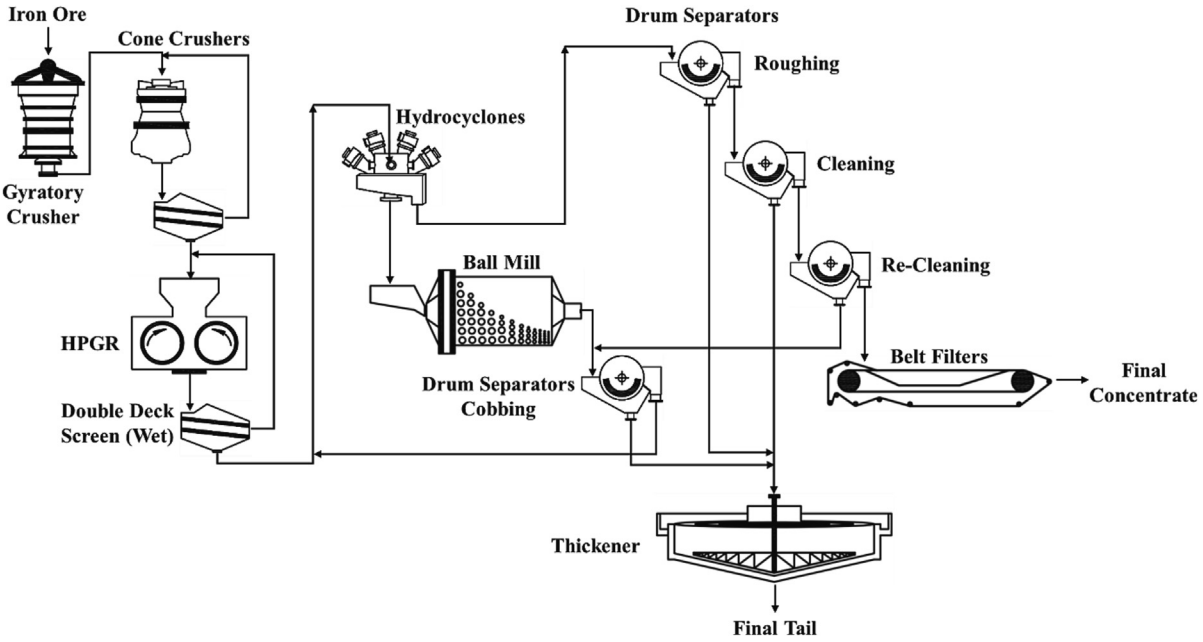

Fig. 1. The flowsheet of iron ore processing plant, Gohar Zamin Iron Ore Company (Kerman, Iran).

2.2. Sample preparation and characterization

About 800 kg the iron ore concentrate was prepared from the iron ore processing plant within a month. It was divided into two equal portions after homogenization. One portion was reserved to implement the proposed strategy and separate the different size fractions. For sample characterization, the other portion was riffled to prepare the representative sub-samples by using a sample divider (PT 600, Retsch GmbH, Haan, Germany). The representative sub-samples for the elemental composition analysis and the phase identification were ground by a vibratory disc mill (Retsch, RS 200). The elemental composition was measured by the x-ray fluorescence (XRF) spectroscopy technique (ARL 9900, Thermo Fisher Company). It's noticeable that the sulfur percentage was measured by Carbon / Sulfur Analyzer ELEMENTRAC CS-i (ELTRA GmbH). The phase identification was done by X-ray powder diffraction (XRD) system (Philips-Xpert Pro). A representative sub-sample was used for the examination and analysis of the sample morphology by scanning electron microscope (SEM, TESCAN). Moreover, controlling the particle size distribution of the samples in the repetition tests and ensuring the similarity of them was done using a CAMSIZER®P4 (Microtrac Retsch GmbH).

2.3. The method of measuring the Blaine number in the laboratory

Measuring the Blaine number by Blaine meter is performed according to ISO 21283 [16], which is based on the time required to pass a certain volume of air through a packed bed of particles with given size and porosity. A schematic view of the Blaine meter and its components is shown in Fig. 2. The method of measuring the Blaine number of iron ore concentrate in the laboratory consists of four consecutive steps [16] (Fig. 3): (1) the sample preparation; (2) the measurement of sample density; (3) the determination of sample mass; and (4) the measurement of Blaine number. Sampling and preparation of a test sample are performed in accordance with ISO 3082 [22].

In the first step, the obtained sample of iron ore concentrate is placed in the oven (Memmert's model variant TwinDISPLAY) to constant its mass at 105 °C ± 5 °C (the difference in mass between two subsequent measurements is less than 0.05 % of the initial mass of sample.). About 300 g representative sample is obtained by a sample divider (PT 600, Retsch GmbH, Haan, Germany). After sieving the representative sample on a 1 mm sieve (Retsch), about 50 g of the minus 1 mm material is obtained by riffling. The obtained sample is disaggregated on a 150 μm sieve. Then, the material retained and passing on the 150 μm sieve is mixed and homogenized. In the second step, the actual density of the prepared sample is measured by a Gas Pycnometer (Micromeritics AccuPyc II 1345). According to ISO 21283 [16], the porosity value of iron ore concentrate is considered to be 0.5. In the third step, the required mass of sample (m_s) for producing a sample bed with the specified porosity (i.e., 0.5) can be calculated as following [16]:

$$m_s = \rho_s V_B (1 - \varepsilon_s) \tag{1}$$

where ε_s is the sample bed porosity (ratio of the volume of voids in the bed to the bulk volume of the bed sample [16]), ρ_s is the sample density (g cm^{-3}), and V_B is the bulk volume of the sample compacted bed (cm^3). In the final step, the Blaine number is measured using a Blaine meter (Model 7201, Toni Technik Baustoffprüfsysteme GmbH). In order to calculate the Blaine number, according to ISO 21283 [16], the equipment constant must first be determined using a Certified Reference Material (CRM; e.g., NIST 114q Portland cement).

For this work, the permeability cell containing the CRM bed is attached to the manometer tube. Using the rubber pear, the air is slowly evacuated in one arm of the U-tube manometer until the liquid reaches the α line, and then the valve is tightly closed, enabling the liquid column to go down. The liquid is allowed for 30 s to run down the walls and then the pressure device is withdrawn, enabling the liquid column to go down. The timer is started when the bottom of the meniscus of the manometer liquid reaches the β line and stopped when the bottom of the meniscus of liquid reaches the γ line. This time interval and the temperature of the test are recorded. At least three determinations of the time interval are conducted (keeping the same compacted bed) and computed

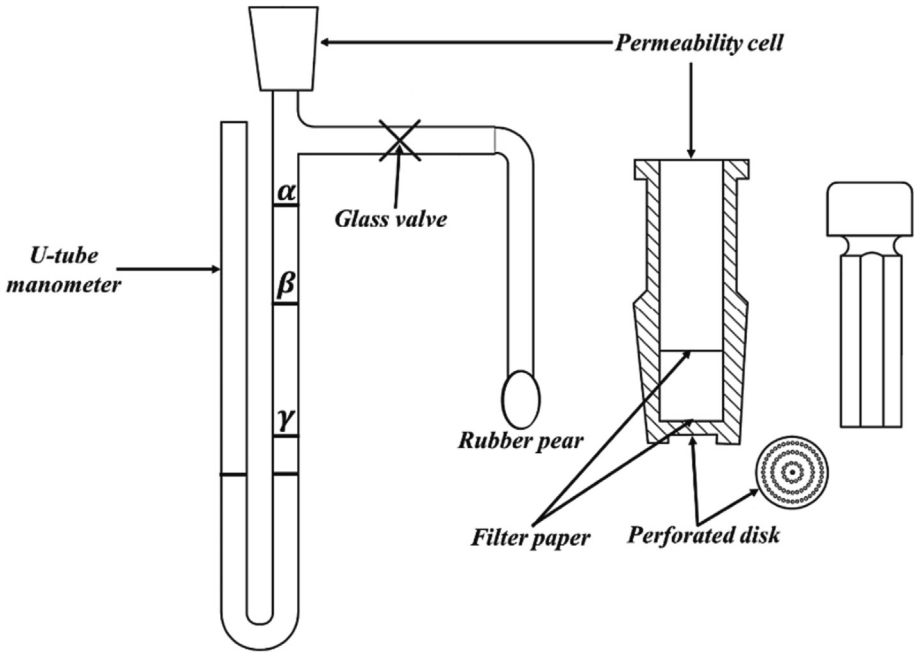

Fig. 2. A schematic view of the Blaine meter and its components; The accurately weighed mass of sample is poured into the permeability cell and compacted with a plunger to produce a packed bed with the desired porosity. The air is slowly evacuated until the liquid reaches the α line, and then the valve is tightly closed. The timer is started when the bottom of the meniscus of the manometer liquid reaches the β line and stopped when it reaches the γ line.

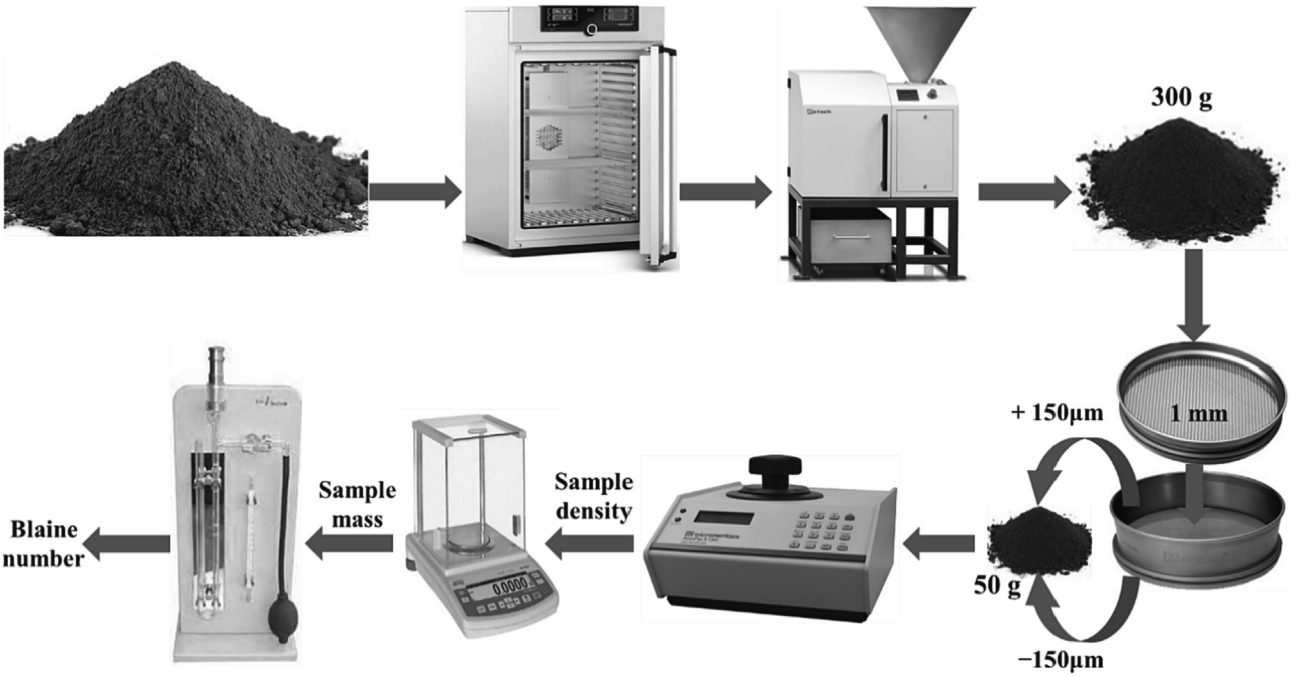

Fig. 3. The steps of measuring the Blaine number in the laboratory according to ISO 21283.

their arithmetic mean. The equipment constant, K, is calculated as following [16]:

$$K = \frac{B_c \rho_c (1-\varepsilon_c)\sqrt{\mu_c}}{\sqrt{\varepsilon_c^3 t_c}} \tag{2}$$

where B_c is the certified Blaine number of the CRM ($cm^2\ g^{-1}$), ρ_c is the CRM density ($g\ cm^{-3}$), ε_c is the CRM porosity (i.e., 0.5), μ_c is the viscosity of air at the temperature of test (µPa s), and t_c is the measured time interval of the liquid column drop in the manometer arm (s). After determining the equipment constant and repeating the previous three steps for sample, the Blaine number of sample, B_s, is calculated as following equation [16]:

$$B_s = \frac{K}{\rho_s(1-\varepsilon_s)}\sqrt{\frac{\varepsilon_s^3 t_s}{\mu_s}} \tag{3}$$

where μ_s is the viscosity of air at the temperature of test (µPa s), and t_s is the measured time interval of the liquid drop in the manometer arm (s). It's noticeable that, in the present study, all Blaine tests were performed with three repetitions and the maximum allowable repeatability of 30 $cm^2\ g^{-1}$ (ISO 21283).

2.4. The proposed strategy for modelling the Blaine number

As mentioned in the section of sample preparation and characterization, about 400 kg the iron ore concentrate was prepared as representative. According to ISO 21283 [16], the proposed strategy should be carried out on the materials passing through the 1 mm sieve. As mentioned in the introduction section, according to the literature [10,13,14], the particle size distribution and the shape are the most important parameters controlling the Blaine number of iron ore concentrate. In the literature [15,19,20], there are some models for describing the relationship between the particle size distribution and the Blaine number of cement particles (B_c) with regular geometric shapes. Kuhlmann (1984) proposed Eq. (4) as following:

$$B_C = \frac{6}{\rho}\sum_{i=1}^{n}\frac{\Delta Q_i(x_i, x_{i+1})}{d_i} \tag{4}$$

where ρ is the cement density ($g\ cm^{-3}$), d_i is the geometric mean size of x_i and x_{i+1} (cm), $\Delta Q_i\ (x_i, x_{i+1})$ is the difference of the cumulative mass distribution of the i^{th} and $(i+1)^{th}$ particle size (%), and n is the number of size fractions. Sumner et al. (1989), proposed Eq. (5) as following:

$$B_C = \frac{6}{\rho}\sum_{i=1}^{n}\left(\frac{w_i F}{100 d_i}\right) \tag{5}$$

where w_i is the weight percentage in size fraction i and F is the surface shape factor (between 1.1 and 1.15). Zhang and Napier-Munn [15] proposed Eq. (6) as following:

$$B_C = \frac{6}{\rho}\sum_{i=1}^{n}\left(\frac{w_i}{x_h}\right) \tag{6}$$

where x_h is a harmonic mean size of x_i and x_{i+1} (cm), which calculated by Eq. (7) [15]:

$$x_h = \sqrt[3]{\frac{(x_{i+1}^2 + x_i^2)(x_{i+1} + x_i)}{4}} \tag{7}$$

According to the hypothesis presented in the proposed strategy, it is assumed that the Blaine number of the iron ore concentrate sample is a function of the Blaine number of the different particle size fractions that make up the overall sample (Each fraction is assumed as a particle). Here, a variable of Blaine number type is defined for each particle size fraction based on two mentioned parameters controlling the Blaine number. The mathematical expression of the proposed hypothesis is as follows:

$$\begin{aligned} B_i &= Volumeshapefactor \times (Particlesize)^2 \\ &= \left(\frac{V_i}{\left(d_{50}^{(-d_{i-1},+d_i)}\right)^3}\right) \times \left(d_{50}^{(-d_{i-1},+d_i)}\right)^2 = \frac{V_i}{d_{50}^{(-d_{i-1},+d_i)}} \\ &= \frac{m_i}{\rho_i d_{50}^{(-d_{i-1},+d_i)}} \forall i = 1ton+1, d_{i-1} > d_i \end{aligned} \tag{8}$$

$$B_{Sample} = f(B_i)\forall i = 1ton+1 \tag{9}$$

where "i" is the sieve number or fraction, B_{Sample} is the Blaine number of iron ore concentrate sample ($cm^2\ g^{-1}$), B_i is the Blain number of remaining materials on the i^{th} sieve ($cm^2\ g^{-1}$), V_i is the volume of remaining materials on the i^{th} sieve (cm^{-3}), m_i is the mass fraction of i^{th} sieve or the mass fraction of remaining materials on the i^{th} sieve, ρ_i is the actual density of remaining materials on the i^{th} sieve ($g\ cm^{-3}$), and $d_{50}^{(-d_i,+d_i)}$ is the average particle size of materials passing through the $(i-1)^{th}$ sieve and remaining on the i^{th} sieve. Here, to simplify the model, it is assumed that this value is equal to the geometric mean size of two consecutive sieves. But for the first and the final sieves, this value should be measured (e.g., using a CAMSIZER®P4).

As can be seen, the particle size distribution is incorporated into the proposed strategy. On the other hand, usually, the particles shape is irregular and does not follow the well-known geometric shapes. Therefore, the volume shape factor was used in the proposed strategy, which is defined as dividing the volume by the cubic mean diameter of each particle [23–26]. It's noticeable that the previously proposed models [15,19,20] are based on the cement particles with regular geometric shapes, while in the proposed strategy, the particles do not necessarily have a regular geometric shape. Also, the form of the previously proposed models [15,19,20] is based on linear regression, while in Eq. (9), a function with an uncertain form is proposed for the Blaine number which is determined by statistical methods. The proposed strategy for modelling the Blaine number consists of several consecutive steps (Fig. 4):

(1) Passing the representative sample (about 400 kg) through a 1 mm sieve and dividing the passing particles into different particle size fractions: according to the manual of Gas Pycnometer [27], the mass fractions (the materials mass remaining on each sieve) should be equal to 2/3 of the pycnometer cell volume ($m^{(-d_{i-1},+d_i)} \propto \frac{2}{3} Volume_{Cell}^{Pyc.}$);

(2) Measuring the actual density of each sample fraction (ρ_i) by a Gas Pycnometer (Micromeritics AccuPyc II 1345);

(3) Making an industrial dataset for the Blaine number of each sample fraction: usually, there is a comprehensive dataset of particle size distribution for the iron ore concentrate in the laboratory of the iron ore processing plant over several consecutive years. Therefore, by using Eq. (8) and the data of the previous step (step 2), it is possible to calculate the Blaine number for each fraction and, as a result, obtain a comprehensive industrial dataset. The Blaine number of each fraction is the input variable for the design of experiments;

(4) Determining the variation range of the Blaine number of each sample fraction based on the industrial dataset (step 3);

(5) The design of experiments (DOE): DOE is a powerful statistical technique for evaluating the effect of parameters and their mutual interactions on the responses of experiments [28–30]. One of DOE methods is the response surface method (RSM), which uses the optimization techniques, the regression analyses and the local regression models to find a suitable functional relationship between the independent variables affecting the process (input variables or factors) and a response. The use of this method has been widely accepted by engineers in various fields due to the acceptable performance in solving the complex and multi-purpose problems [31,32].

The most popular RSM design is the central composite design (CCD) which is a five-level RSM design. For a CCD, three groups of design points are needed: (a) the two-level factorial or fractional factorial design (i.e., a statistical experimental design used to investigate the effects of two or more independent variables on a dependent variable [33]) points which are coded as ± 1; (b) the axial or star points at the distances ± α from experimental points centers; and (c) the center point which is coded as 0. In other words, five levels are defined for each factor as ($-\alpha$, −1, 0, +1, $+\alpha$).

There are different options in this design, i.e., the factorial core of CCD, based on the number of factors included in the experiment. The default option is the largest fraction that will result in the production of a design under 1000 runs or maintain at least resolution V behavior [29,34–36]. Therefore, for six or more factors, the Minimum runs resolution-V type (Min Run Res V), i.e., a smaller fractional core, is recommended to save time and money and get the good estimates with keeping the number of runs under control [29,34–36].

(6) The analysis of variance (ANOVA): the basis of ANOVA is the law of total variance, where the observed variance in a special variable is partitioned into components attributable to different variation sources. In this step, the differences among means are analyzed by using the statistical models and their associated esti-

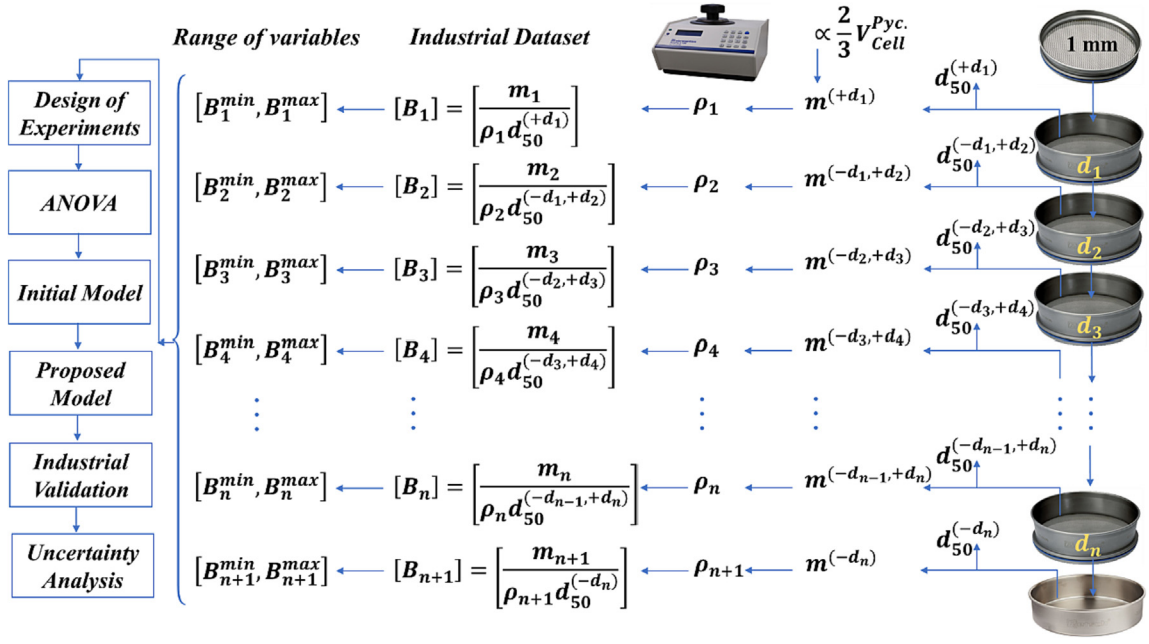

Fig. 4. The proposed strategy for modelling the Blaine number of iron ore concentrate.

mation procedures. The used models are included the fixed-effects models, the random-effects models and the mixed-effects models. The fixed-effects models are used when one or more treatments to the subjects of the experiment is applied to investigate the change of the response variable values and consequently, to estimate the range of response variable values that the treatment would generate in the population as a whole [37].

The random-effects models are used when the various factor levels are sampled from a larger population and consequently, the treatments are not fixed. The mixed-effects models contain experimental factors of both fixed and random-effects types [37]. In this study, the investigated parameters of ANOVA include P-value (i.e., the probability under the assumption of no effect or no difference (null hypothesis), of obtaining a result equal to or more extreme than what was actually observed [35]), F-value (i.e., a value on the F distribution [35]), the predicted residual error sum of squares (*PRESS*), the mean sum of squares of error (*MSE*), the R-squared (R^2), the adjusted R-squared (R^2_{adj}), and the predicted R-squared (R^2_{pre}). The R^2_{adj} and the R^2_{pre} should be within approximately 0.20 of each other to be in reasonable agreement [28,29,37].

(7) Determining the initial model: the appropriate initial model is statistically determined by comparing the ANOVA (Analysis of variance) parameters (the step (6)) of the regression models in the RSM (Eqs. (10) to (13)). In other words, in this step, the appropriate model form is determined from among the regression models of RSM.

(8) Presentation of the proposed model: a set of adjustments and the different scenarios are applied on the selected initial model based on analysis of variance to improve the accuracy of ANOVA parameters (the previous step parameters) and the variance inflation factor (*VIF*). The *VIF* measures the upsurge of the variance in comparison with an orthogonal basis and its value for i^{th} variable is calculated as following [38,39]:

$$VIF_i = \frac{1}{1 - R_i^2} \tag{10}$$

where R_i^2 is the coefficient of determination obtained by regressing the i^{th} predictor on the remaining predictors.

(9) The industrial validation: the proposed model for estimation of the Blaine number is validated with the industrial data.

(10) The model sensitivity and reliability analysis under uncertainty: In the experiments, the measurement errors resulting from different sources (e.g., systematic error, human error, random error, etc.) can lead to uncertainty in calculations and results [40–42]. Therefore, the probabilistic and the reliability analysis under uncertainty is necessary for data validation, calculations, and results [43–45]. One of the best methods of the probabilistic and the reliability analysis is the Monte Carlo simulation [46,47], which simulates the final function using a series of random numbers from the probability distribution of the variables and solves the highly complicated problems with nondeterministic nature [48,49]. The Monte Carlo simulation is used in many studies due to the shorter duration, the possibility of optimizing the function, the simplicity and ease of use, its conformity to different types of functions, and the lack of need for boundary conditions [43,50–53]. In the present study, the Monte Carlo simulation was implemented using @RISK software in Excel to analyze the proposed model under uncertainty.

The Monte Carlo simulation consists of five steps: (1) Determining the suitable deterministic solver (the suitable regression model); (2) Determining the input variables for the probabilistic modeling and quantifying the variations; (3) The random sampling for each parameter by applying the probability density function: Each sample is randomly selected from the range of input data distribution [49,54]. The performance distribution function and the failure probability are determined by applying the output data. In a Monte Carlo simulation, subsequent calculations are carried out by using numbers, which are generated for each parameter based on the probability distribution functions (e.g., the normal distribution, the Poisson distribution, and the log-normal distribution). In the Monte Carlo simulation, usually, the stability of the final results is obtained with more iterations (e.g., 10,000 iterations) [49,54]; (4) Solving the problem by applying the deterministic analysis, and (5) Repeating steps (3) and (4) until an adequate number of simulations is obtained.

2.5. The method of using the proposed model for unknown samples

To use the obtained model for unknown samples, several steps must be done (Fig. 5): (1) Measuring the actual density of the sam-

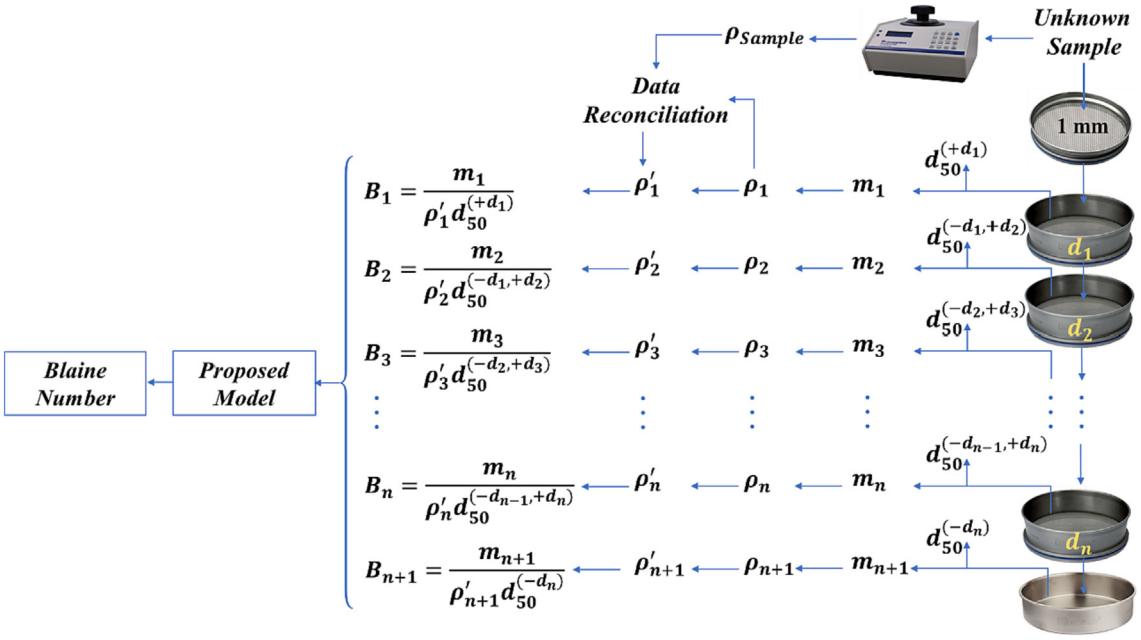

Fig. 5. The method of using the proposed model for unknown samples.

ple (ρ) by a Gas Pycnometer; (2) Determining the particle size distribution of the sample and the mass fractions (m_i); (3) Reconciling the actual density of each sample fraction (ρ_i) with the data reconciliation technique and the values of ρ and m_i: the data reconciliation is a widely used technique to calculate the unmeasured variables and increase the accuracy of the measured variables by an optimization approach and minimizing the objective function. If the reconciled values for the actual density of each sample fraction are displayed as $\hat{\rho}_i$, the mathematical expression of the data reconciliation technique can be written as follows [55,56]:

$$\min_{\hat{\rho}_i} \left(\rho - \frac{\sum_{i=1}^{n} \left(m_i \hat{\rho}_i \right)}{\sum_{i=1}^{n} m_i} \right)^2 \text{ by changing } \rho_i \text{subject to } \hat{\rho}_i > 0 \qquad (11)$$

where n is the number of sieves used in the particle size analysis. Usually, the Eq. (11) is solved by the fmincon solver in MATLAB or the solver in Excel; (4) Placing the reconciled values for the actual density of each sample fraction in the proposed model and calculating the Blaine number.

3. Results and discussion

3.1. Sample characterization

In Fig. 6 (Left), the XRD results showed that the dominant mineral in the iron ore concentrate is magnetite (Fe_3O_4) with a small amount of clinochlore (Mg_5Al ($AlSi_3O_{10}$) $(OH)_8$), quartz (SiO_2) and pyrite (FeS_2). The Fig. 6 (Right) is the analysis of the sample morphology by scanning electron microscope (SEM). The SEM results showed that the particles don't have a regular geometric shape.

3.2. Modelling the Blaine number by the proposed strategy

As mentioned in the section of materials and methods, the proposed strategy for modelling the Blaine number consists of 10 steps. The results of each stage are as follows:

(1) Passing the representative sample (about 400 kg) through a 1 mm sieve and dividing the passing particles into different particle size fractions by sieves of 500 μm, 355 μm, 250 μm, 180 μm, 125 μm, 90 μm, 63 μm, 45 μm and –45 μm (under 45 μm).

(2) Measuring the actual density of each sample fraction with 4 repetitions (Table 1): The accuracy of the measured values was confirmed by establishing the equation $\frac{\sum_{i=1}^{n} m_i \rho_i}{\sum_{i=1}^{n} m_i} = \rho_{sample}$. ρ_{sample} is the actual density of the overall sample passing through the 1 mm sieve.

(3) Making an industrial dataset for the Blaine number of each sample fraction by using a comprehensive dataset of particle size distribution for the iron ore concentrate in the laboratory of the iron ore processing plant, Eq. (8) and the obtained actual density for each sample fraction. In Eq. (8), it's noticeable that d_{50} for each sample fraction is equal to the geometric mean size of two consecutive sieves (Table 1); for example, d_{50} for the particle size fraction of (+355 –500) is considered equal to 421.3 μm. For the particle size fractions of (+500 μm) and (–45 μm), d_{50} were measured by using a CAMSIZER®P4 that their values were equal to about 506 μm and 21 μm. Therefore, for simplicity, their values were considered equal to 500 μm and 22.5 μm.

(4) Determining the variation range of variables (the Blaine number of each sample fraction) based on the industrial dataset obtained in the step 3 and normalizing the variables (Table 2).

(5) Design of experiments: The five-level nine-variable CCD and the Minimum runs resolution-V type (Min Run Res V) is designed to describe the response surfaces with 64 experiments and 6 repetitions with central points. To prepare the sample required for each designed experiment, first m_i (mass) was calculated for each variable by Eq. (8). Then, m_s (the required sample mass for measuring the Blaine number) was calculated by Eq. (1). It was observed that the value of $\sum_{i=1}^{n} m_i$ is not equal to the value of m_s. Therefore, the value of m_i for each variable was modified (m_i') by using the ratio of $\frac{m_i m_s}{\sum_{i=1}^{n} m_i}$ so that $\sum_{i=1}^{n} m_i' = m_s$. It is important to mention that for each experiment, three samples were prepared to ensure the high accuracy of Blaine number measurement. Moreover, the similarity of samples in terms of particle size distribution was evaluated and controlled using a CAMSIZER®P4. After preparing the samples, their Blaine number was measured. The part of CCD with the coded/actual values (input variables) and the results of Blaine number were given in Table 3.

(6) The analysis of variance (ANOVA): In order to construct the linear, 2FI, quadratic, and cubic response surfaces of the Blaine number, the output of the RSM models were statistically analyzed and the parameters of ANOVA were calculated (Table 4).

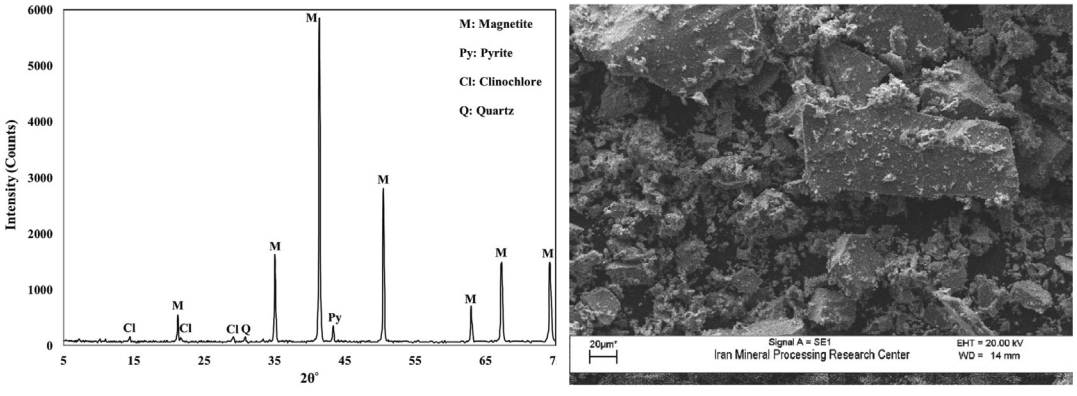

Fig. 6. (Left) XRD and (Right) SEM of iron ore concentrate obtained from the iron ore processing plant of Gohar Zamin Iron Ore Company, Sirjan-Iran.

Table 1
The actual density and d_{50} of each sample fraction.

Particle size fraction (μm)	+500	+355–500	+250–355	+180–250	+125–180	+90–125	+63–90	+45–63	–45
d_{50} (μm)	500	421.3	297.9	212.1	150.0	106.1	75.3	53.2	22.5
Actual density ρ_i (g cm^{-3})	3.83	3.81	4.17	4.78	4.99	5.00	5.00	4.99	4.94

Table 2
Coded and actual levels of input variables (the variation range of variables).

Particle size fraction (μm)	Variable ($cm^2\ g^{-1}$)	−α	−1	0	+1	+α
+500	B_1	0.00	0.10	0.20	0.30	0.40
+355–500	B_2	0.00	0.03	0.05	0.07	0.10
+250–355	B_3	0.00	0.07	0.15	0.23	0.30
+180–250	B_4	0.10	0.25	0.40	0.55	0.70
+125–180	B_5	0.30	0.92	1.55	2.17	2.80
+90–125	B_6	0.40	1.67	2.95	4.22	5.50
+63–90	B_7	0.40	2.62	4.85	7.07	9.30
+45–63	B_8	0.00	1.83	3.65	5.47	7.30
−45	B_9	21.70	31.00	40.30	49.60	58.90

(7) Determining the initial model: As seen in Table 4, the values of R-squared for the RSM models of linear, 2FI, quadratic and cubic are 0.6474, 0.9926, 0.9976, and 0.9993, respectively. Obviously, the linear model is not the suitable model to estimate the Blaine number. By comparing the R^2_{adj} and the R^2_{pre} of the remaining models, it's found that their difference for the models of 2FI and cubic is more than 0.2. Therefore, the appropriate initial model is the quadratic, which for the present work was written as following:

$$\begin{aligned} Blainenumber_{Quadratic} = {} & 917.04 - 823.18B1 - 8580.06B2 \\ & + 1699.87B3 + 1414.77B4 \\ & - 154.95B5 - 67.76B6 - 139.49B7 \\ & + 46.56B8 + 22.23B9 + 10598.85B1 \\ & \times B2 - 1896.72B1 \times B3 - 4088.99B1 \\ & \times B4 + 766.72B1 \times B5 + 167.31B1 \\ & \times B6 + 226.66B1 \times B7 - 142.60B1 \\ & \times B8 - 2.42B1 \times B9 - 7771.88B2 \\ & \times B3 + 10125.42B2 \times B4 - 976.18B2 \\ & \times B5 + 1232.55B2 \times B6 + 40.82B2 \\ & \times B7 + 670.43B2 \times B8 - 40.67B2 \\ & \times B9 + 268.84B3 \times B4 - 993.61B3 \\ & \times B5 - 439.83B3 \times B6 + 268.98B3 \\ & \times B7 - 299.41B3 \times B8 + 38.54B3 \\ & \times B9 - 259.70B4 \times B5 - 171.56B4 \\ & \times B6 + 3.56B4 \times B7 - 74.79B4 \times B8 \\ & - 3.65B4 \times B9 + 13.92B5 \times B6 \\ & + 5.99B5 \times B7 + 23.54B5 \times B8 \\ & + 0.26B5 \times B9 - 0.13B6 \times B7 \\ & - 0.79B6 \times B8 + 0.69B6 \times B9 \\ & - 4.16B7 \times B8 + 0.85B7 \times B9 \\ & - 0.34B8 \times B9 + 20.95(B1)^2 \\ & + 1935.26(B2)^2 - 873.86(B3)^2 \\ & + 70.42(B4)^2 + 29.66(B5)^2 \\ & - 0.56(B6)^2 - 0.01(B7)^2 + 1.49(B8)^2 \\ & - 0.17(B9)^2 \end{aligned} \quad (12)$$

(8) Presentation of the proposed model: By removing some not-significant (p-value > 0.05) parameters of the quadratic model (Eq. (12)) and controlling the variance inflation factor (*VIF*), simultaneously, the proposed model for the estimation of the Blaine number ($cm^2\ g^{-1}$) can be written as Eq. (13):

$$\begin{aligned} Blainenumber = {} & 941.88 - 914.82B1 - 8322.40B2 \\ & + 1365.69B3 + 1359.41B4 - 154.06B5 \\ & - 38.97B6 - 136.93B7 + 50.80B8 \\ & + 20.31B9 + 10904.39B1 \times B2 \\ & - 1590.50B1 \times B3 - 4161.46B1 \times B4 \\ & + 770.40B1 \times B5 + 173.50B1 \times B6 \\ & + 219.14B1 \times B7 - 147.43B1 \times B8 \\ & - 7002.38B2 \times B3 + 10447.69B2 \times B4 \\ & - 899.18B2 \times B5 + 1199.57B2 \times B6 \\ & + 655.99B2 \times B8 - 44.21B2 \times B9 \\ & - 1014.51B3 \times B5 - 436.96B3 \times B6 \\ & + 258.80B3 \times B7 - 296.40B3 \times B8 \\ & + 41.77B3 \times B9 - 228.93B4 \times B5 \\ & - 176.48B4 \times B6 - 79.49B4 \times B8 \\ & + 10.37B5 \times B6 + 7.40B5 \times B7 + 22.66B5 \\ & \times B8 - 5.23B7 \times B8 + 0.97B7 \times B9 \\ & + 30.28(B5)^2 - 0.17(B9)^2 \end{aligned} \quad (13)$$

The results of ANOVA and the *VIF* of parameters were presented in Table 5. According to the results of ANOVA, the p-value of the proposed model is less than 0.05 (<0.0001), which means a high accuracy for the prediction of Blaine number. Moreover, the values of F-value and p-value for lack of fit are 1.08 and 0.5214, respectively. Therefore, the proposed model can be very satisfactory. Based on the values of F-value and p-value, the B_9 is the most effective parameter influencing the Blaine number of iron ore concentrate. According to Table 2, the B_9 is the representative of the Blaine number of particles belonging to the particle size fraction under 45 μm (−45 μm). Accordingly, this parameter can play the most important role on the Blaine number of total sample due to the high mass of particles belonging to this fraction in the total sample (more than 30 %), having the highest specific surface area of particles in this particle size fraction, the smallest particle dimensions and as a result, reducing porosity and increasing the air passage time along the cell of the Blaine meter.

According to Table 5, the B_1 and the B_2 don't have a significant effect on the Blaine number of total sample. According to Table 2, the B_1 and the B_2 are the representative of the Blaine number of particles belonging to the particle size fraction over 500 μm (+500 μm) and + 355–500 μm, respectively. The non-significant effect of these parameters can be due to the low mass of particles belonging to these fractions in the total sample (less than 0.5 %). It is necessary to explain, although these particles alone do not have a significant effect on the Blaine number of total sample, but their presence together with other particles has a significant effect on the porosity and the Blaine number of total sample (Table 5). For this reason, the B_1 and the B_2 were not removed from the proposed model.

As seen in Table 5, the *VIF* of parameters are less than 2, presenting a high goodness of fit for the proposed model. Generally, the *VIF* more than five can indicate a severe multi–collinearity. The other parameters of ANOVA for the proposed model are: Degree of freedom (*df*) = 37, MSE = 71037.67, Adequate precision = 54.74, *PRESS* = 75380.04, R^2 = 0.9953, R^2_{adj} = 0.9900, and R^2_{pre} = 0.9715. As seen, the obtained results for the proposed model, compared to the quadratic model (Eq. (12)), indicate the higher accuracy of the proposed model.

Fig. 7 is a perturbation plot which illustrates the effect of all the factors at the center point in the design space. It is evident from

Table 3
Part of CCD consisting of the nine input variables (coded) and the results of Blaine number.

Run no.	Input variables (cm^2g^{-1})									Response (cm^2g^{-1})
	B_1	B_2	B_3	B_4	B_5	B_6	B_7	B_8	B_9	Blaine number
1	-α	0	0	0	0	0	0	0	0	1066
2	0	0	0	0	0	-α	0	0	0	1217
3	0	0	0	0	0	0	0	0	-α	701
4	+1	+1	−1	−1	−1	+1	+1	−1	−1	941
5	−1	+1	−1	−1	−1	+1	+1	−1	+1	923
6	+1	+1	+1	+1	+1	−1	+1	−1	−1	948
7	+1	−1	−1	+1	+1	−1	−1	−1	−1	1018
8	0	0	0	0	0	α	0	0	0	865
9	+1	+1	−1	+1	+1	−1	−1	+1	+1	1250
10	+1	−1	−1	−1	−1	−1	+1	+1	−1	855
11	0	0	0	0	-α	0	0	0	0	1151
12	+1	+1	+1	+1	+1	+1	−1	−1	−1	630
13	+1	−1	+1	+1	+1	+1	−1	+1	+1	705
14	−1	+1	+1	−1	+1	−1	−1	+1	+1	1100
15	−1	+1	−1	−1	+1	−1	+1	+1	+1	1012
16	0	0	0	0	0	0	0	-α	0	1120
17	0	0	0	0	0	0	α	0	0	938
18	−1	−1	−1	−1	+1	+1	−1	+1	+1	1372
19	0	0	0	0	α	0	0	0	0	1031
20	0	0	0	0	0	0	0	0	0	1094
21	0	α	0	0	0	0	0	0	0	1058
22	0	0	0	-α	0	0	0	0	0	1078
23	0	0	0	0	0	0	0	0	0	1062
24	+1	−1	−1	+1	−1	+1	−1	+1	−1	658
25	−1	−1	+1	−1	+1	+1	−1	−1	−1	736
26	0	-α	0	0	0	0	0	0	0	1041
27	−1	−1	−1	+1	+1	+1	+1	−1	+1	940
28	+1	−1	+1	−1	+1	−1	+1	+1	+1	1389
29	0	0	0	0	0	0	0	0	0	1076
30	0	0	0	0	0	0	-α	0	0	1151
31	+1	+1	+1	+1	−1	−1	−1	+1	−1	902
32	−1	+1	+1	+1	+1	−1	−1	+1	−1	990
33	−1	−1	−1	+1	−1	+1	+1	+1	+1	918
34	+1	+1	+1	−1	−1	−1	+1	−1	+1	1401
35	0	0	0	0	0	0	0	0	0	1045
36	+1	−1	−1	+1	−1	−1	+1	−1	+1	1156
37	−1	−1	+1	−1	+1	−1	+1	−1	−1	923
38	−1	−1	−1	−1	−1	−1	−1	−1	−1	1167
39	−1	+1	+1	−1	−1	−1	−1	−1	−1	1019
40	+1	−1	+1	+1	+1	+1	+1	−1	−1	680
41	−1	−1	+1	−1	−1	+1	+1	−1	+1	1250
42	0	0	0	0	0	0	0	0	α	1268
43	+1	+1	−1	−1	−1	+1	−1	+1	+1	1306
44	0	0	0	0	0	0	0	α	0	1009
45	−1	−1	+1	+1	+1	+1	+1	+1	+1	827
46	0	0	α	0	0	0	0	0	0	987
47	−1	−1	+1	−1	−1	−1	−1	+1	−1	1190
48	−1	−1	−1	+1	+1	−1	+1	+1	−1	910
49	0	0	-α	0	0	0	0	0	0	1063
50	+1	+1	−1	+1	+1	+1	+1	+1	−1	962
51	−1	+1	−1	+1	−1	−1	−1	−1	+1	1438
52	+1	−1	−1	+1	−1	+1	−1	−1	+1	1006
53	−1	+1	+1	+1	−1	+1	−1	+1	+1	1258
54	+1	+1	+1	−1	−1	+1	+1	+1	−1	805
55	+1	−1	+1	−1	−1	−1	−1	−1	−1	1143
56	0	0	0	0	0	0	0	0	0	1048
57	0	0	0	0	0	0	0	0	0	1052
58	+1	+1	−1	−1	+1	−1	−1	+1	−1	1216
59	+1	+1	+1	−1	+1	+1	+1	−1	+1	1296
60	−1	+1	−1	+1	−1	+1	+1	+1	−1	856
61	−1	+1	−1	−1	+1	+1	−1	−1	−1	850
62	+1	−1	−1	−1	−1	−1	−1	+1	+1	1223
63	−1	−1	+1	+1	+1	−1	−1	−1	+1	1425
64	−1	−1	+1	+1	−1	+1	+1	−1	−1	866
65	α	0	0	0	0	0	0	0	0	1025
66	−1	−1	−1	−1	+1	+1	+1	+1	−1	785
67	+1	+1	−1	−1	+1	−1	−1	−1	+1	1215
68	+1	+1	+1	+1	−1	+1	+1	−1	+1	1284
69	−1	+1	+1	+1	−1	−1	+1	+1	+1	1430
70	0	0	0	α	0	0	0	0	0	1024

Table 4
The parameters of ANOVA for the RSM models of the Blaine number.

Response surface model	Degree of freedom	MSE	F-value	P-value	Adequate precision	PRESS	R^2	R^2_{adj}	R^2_{pre}
Linear	9	190,000	12.24	< 0.0001	13.65	1,382,000	0.6474	0.5946	0.4766
2FI	45	58246.89	71.43	< 0.0001	34.23	408,100	0.9926	0.9787	0.7551
Quadratic	54	48784.55	115.90	< 0.0001	43.56	646,800	0.9976	0.9890	0.8454
Cubic	61	43259.71	188.35	< 0.0001	55.16	1,020,000	0.9993	0.9940	0.6139

Table 5
Part results of ANOVA and the *VIF* of parameters for the proposed model.

Source	F-value	P-value	*VIF*	Source	F-value	P-value	*VIF*
Propose model	185.03	< 0.0001	–	$B_2 \times B_5$	15.34	0.0004	1.54
B_1	1.73	0.1979	1.44	$B_2 \times B_6$	90.00	< 0.0001	1.94
B_2	3.71	0.0629	1.54	$B_2 \times B_8$	76.06	< 0.0001	1.41
B_3	48.07	< 0.0001	1.55	$B_2 \times B_9$	8.03	0.0079	1.57
B_4	29.12	< 0.0001	1.46	$B_3 \times B_5$	176.75	< 0.0001	1.53
B_5	79.66	< 0.0001	1.44	$B_3 \times B_6$	142.88	< 0.0001	1.46
B_6	666.55	< 0.0001	1.42	$B_3 \times B_7$	143.50	< 0.0001	1.56
B_7	272.56	< 0.0001	1.32	$B_3 \times B_8$	140.33	< 0.0001	1.39
B_8	48.53	< 0.0001	1.48	$B_3 \times B_9$	61.41	< 0.0001	1.65
B_9	2173.13	< 0.0001	1.31	$B_4 \times B_5$	39.02	< 0.0001	1.41
$B_1 \times B_2$	59.13	< 0.0001	1.49	$B_4 \times B_6$	96.58	< 0.0001	1.40
$B_1 \times B_3$	11.13	0.0022	1.53	$B_4 \times B_8$	39.14	< 0.0001	1.45
$B_1 \times B_4$	299.37	< 0.0001	1.56	$B_5 \times B_6$	4.81	0.0357	1.70
$B_1 \times B_5$	187.14	< 0.0001	1.48	$B_5 \times B_7$	8.72	0.0059	1.45
$B_1 \times B_6$	33.61	< 0.0001	1.74	$B_5 \times B_8$	50.92	< 0.0001	1.57
$B_1 \times B_7$	167.91	< 0.0001	1.69	$B_7 \times B_8$	38.89	< 0.0001	1.39
$B_1 \times B_8$	60.08	< 0.0001	1.44	$B_7 \times B_9$	32.77	< 0.0001	1.48
$B_2 \times B_3$	12.63	0.0012	1.63	$(B_5)^2$	12.94	0.0011	1.02
$B_2 \times B_4$	106.18	< 0.0001	1.73	$(B_9)^2$	20.26	< 0.0001	1.02
Lack of Fit	1.08	0.5214	–	–	–	–	–

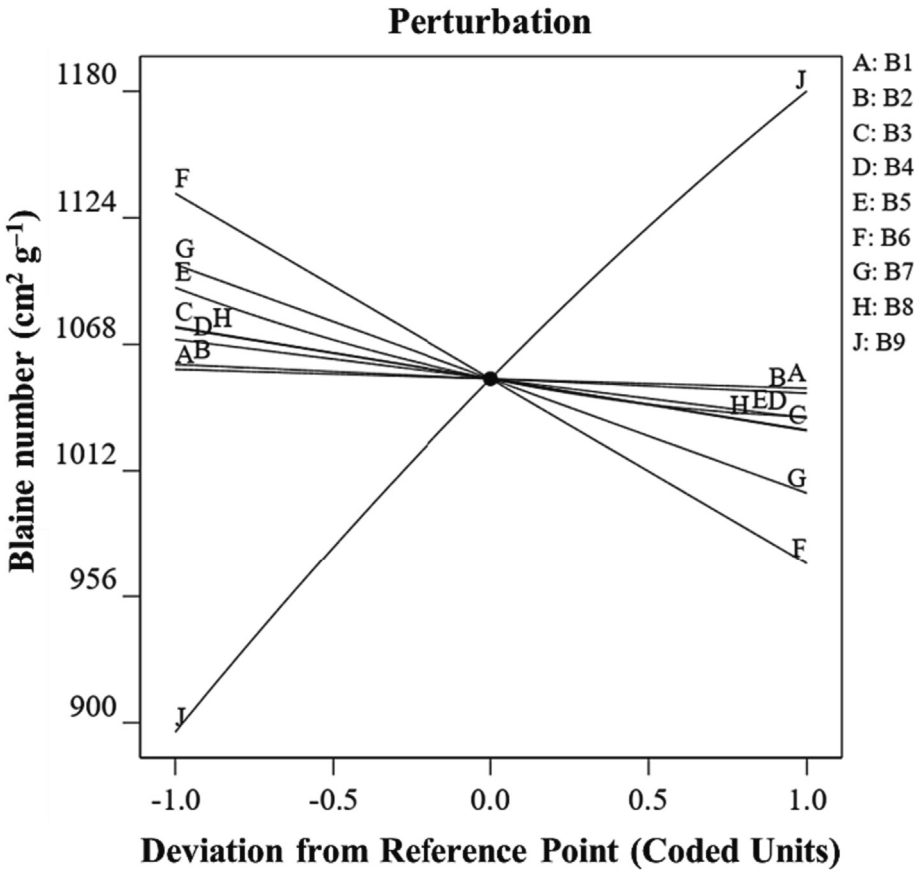

Fig. 7. Perturbation plot showing the effect of all factors on the Blaine number.

Fig. 7 that both the B_1 and the B_2 don't have a significant effect on the Blaine number of total sample. It is apparent that the B_9 (the Blaine number of particles belonging to the particle size fraction under 45 μm) has the significant positive linear effect on the Blaine number of total sample (Fig. 7). This means that the Blaine number of total sample increases as the B_1 level increases, which was in accord with the results reported by Abazarpoor et al. [13] and Hosseini Nasab and Sadeghi [14].

Fig. 8 is the contours plots showing the interaction effects of some variables on the Blaine number, which can be analyzed based on their effect on porosity. For example, Fig. 8a is contours plot illustrating the interaction effect, which is found out only through design of experiments [57], between the B_1 (the representative of the Blaine number of particles + 500 μm) and the B_4 (the representative of the Blaine number of particles + 180–250 μm) on the Blaine number. As seen in Fig. 8a, in the low values of the B_1 (0.10 $cm^2\ g^{-1}$), increasing the B_4 from 0.25 $cm^2\ g^{-1}$ to 0.55 $cm^2\ g^{-1}$ result in a significant increase in Blaine number from about 1012 $cm^2\ g^{-1}$ to 1101 $cm^2\ g^{-1}$. This behavior may be due to the fact that in the presence of low number of coarse particles (+500 μm), an increase in fine particles would result in a significant decrease in porosity and, as a result, an increase in Blaine number. Also, in

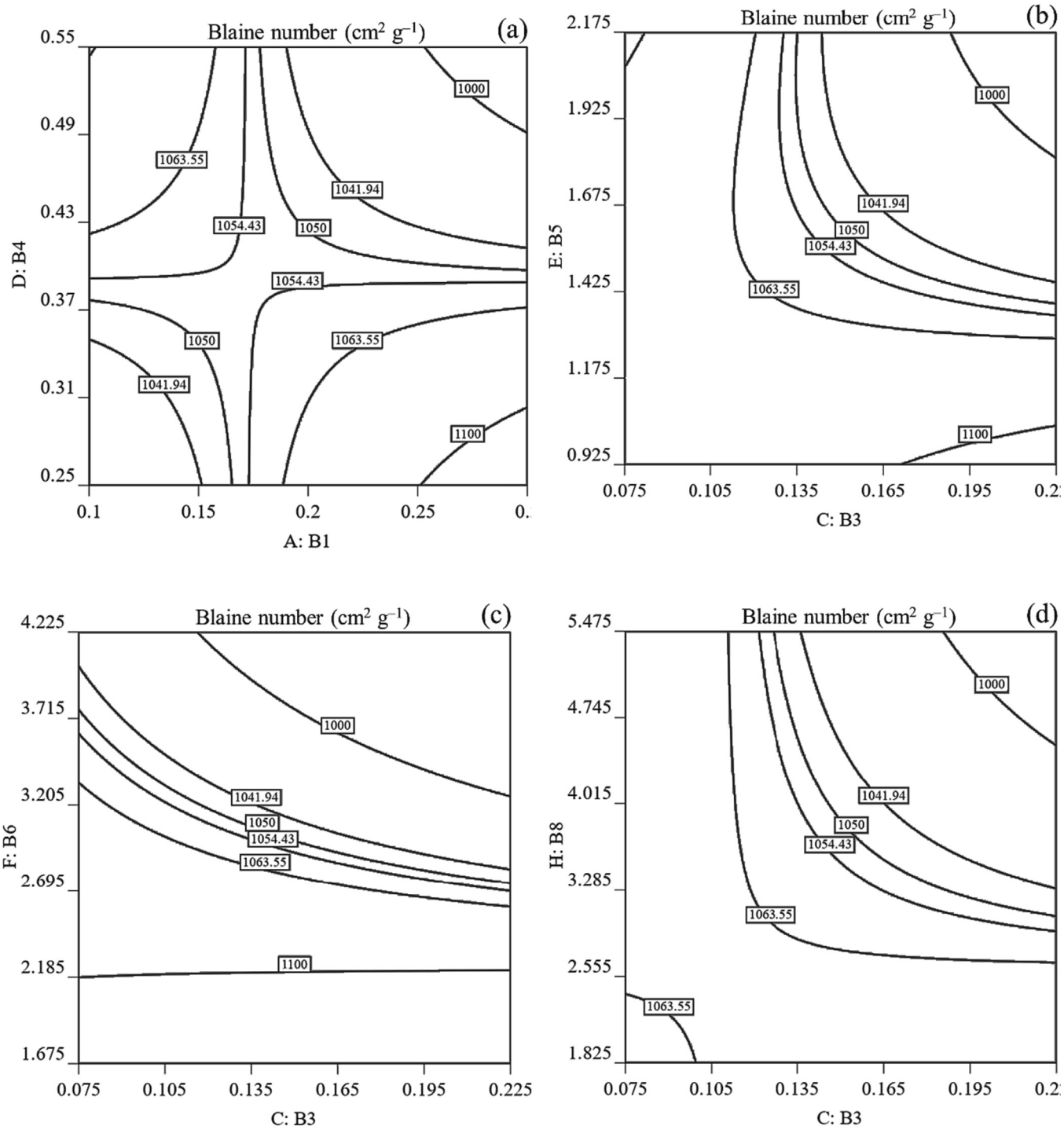

Fig. 8. Contours plots showing interaction effects of (a) B_1 and B_4, (b) B_3 and B_5, (c) B_3 and B_6, and (d) B_3 and B_8 on the Blaine number.

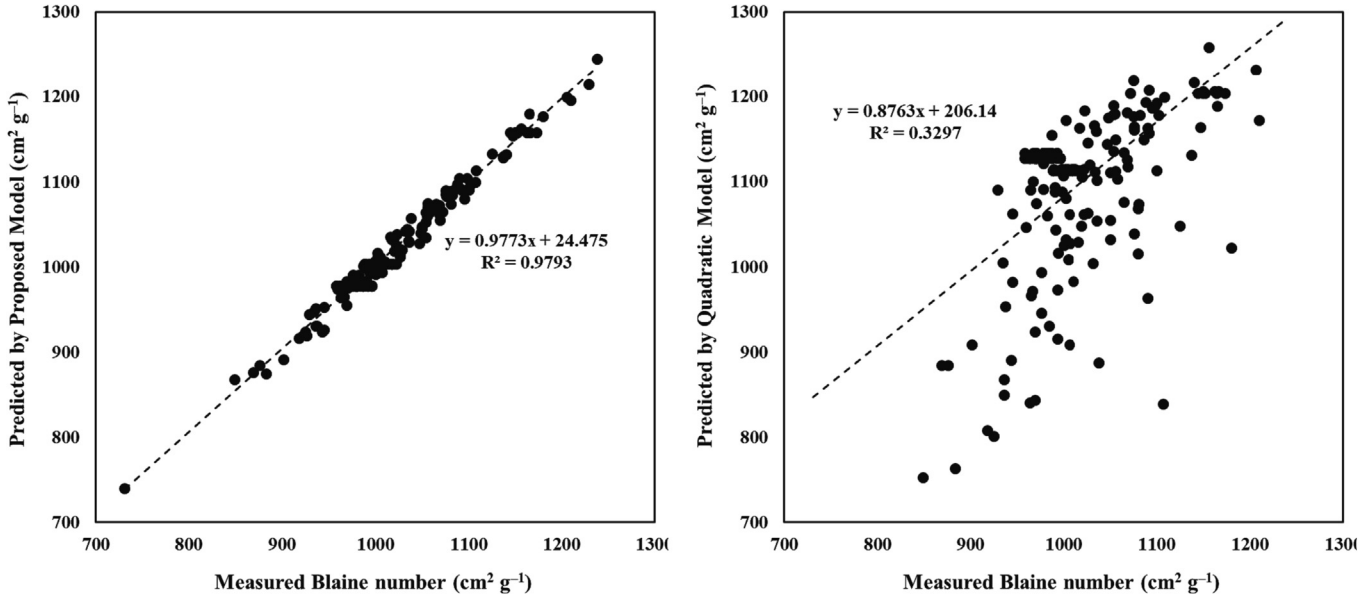

Fig. 9. The comparison of the Blaine number predicted by the proposed model (Left) and the quadratic model (Right).

Table 6
The properties of input parameters in the uncertainty's simulation.

Variable	Probability distribution function	Minimum	Maximum	Mean	Standard deviation	Skewness	Kurtosis
B_1	Loglogistic	0.000	2.195	0.013	0.037	0.001	32.293
B_2	Weibull	0.000	0.053	0.019	0.008	0.000	0.307
B_3	Weibull	0.017	0.181	0.081	0.026	0.001	0.253
B_4	Weibull	0.023	0.582	0.362	0.080	0.006	−0.364
B_5	Weibull	0.337	2.267	1.699	0.238	0.056	−0.977
B_6	Loglogistic	1.954	6.497	2.929	0.290	0.084	1.259
B_7	Loglogistic	2.246	9.365	3.961	0.556	0.309	1.054
B_8	Triangular	0.005	5.822	3.515	1.332	1.774	−0.500
B_9	Loglogistic	25.255	72.422	35.959	2.975	8.850	1.001

the high values of the B_1 (0.30 $cm^2\ g^{-1}$), increasing the B_4 would result in a significant decrease in Blaine number from about 1128 $cm^2\ g^{-1}$ to 970 $cm^2\ g^{-1}$. This behavior may be due to the fact that the presence of high number of coarse particles (+500 μm) would result in an increase in porosity and overcome the positive effect of fine particles on increasing the Blaine number.

(9) The industrial validation: In order to evaluate the validity of the proposed model, it was used for estimating the Blaine number of 228 samples of iron ore concentrate collected from Gohar Zamin Iron Ore Company, Gol-e-Gohar Mining & Industrial Company, and Chadormalu Mining and Industrial Company. It's noticeable that the data for 228 samples, including the particle size distribution, the actual density and the Blaine number, were received from these companies. The proposed model was implemented based on the method introduced in the section of "the method of using the proposed model for unknown samples" and Fig. 5. The comparison of the obtained results of the proposed model and the quadratic model (Eq. (12)) was shown in Fig. 9. As it can be seen, the R-square for the proposed model (i.e., 0.9793) is of priority in relation to the quadratic model (i.e., 0.3297), which shows the high accuracy of the proposed model for estimating the Blaine number of iron ore concentrate.

(10) The model sensitivity analysis under uncertainty: Generally, the measurement errors resulting from different sources can lead to uncertainty in results. The Monte Carlo simulation was used to analyze the reliability of the proposed model for estimating the Blaine number under uncertainty. According to the industrial data (Fig. 9), the type and the properties of the probability distribution function were determined for each significant operational parameter (Table 6). As shown in Table 6, the distribution function of B_1, B_6, B_7, and B_9 is a Loglogistic function, the distribution function of B_2, B_3, B_4, and B_5 is a Weibull function, and the distribution function of B_8 is a Triangular function. Then, the simulation was run by using Eq. (13) with the iteration of 10000. According to Fig. 10, the mean Blaine number is 1011.156 $cm^2\ g^{-1}$ while the values of standard deviation, minimum, and maximum are 51.440, 829.119, and 1611.414 $cm^2\ g^{-1}$, respectively. As seen, the probability distribution function of the Blaine number follows the loglogistic distribution function.

In Fig. 11, the results of probability analysis for the Blaine number were showed. For example, according to Fig. 11, there is a probability of only 2.5 % for the Blaine number to be smaller than or equal to 920 $cm^2\ g^{-1}$ in different experiments. Besides, the values of Blaine number smaller than or equal to 1097 $cm^2\ g^{-1}$ could be obtained with a probability of 95 % in the different experiments. The values of Blaine number smaller than or equal to 1059 $cm^2\ g^{-1}$ could also be obtained with a probability of 85 %. Therefore, the results probability of different tests leading to the values of

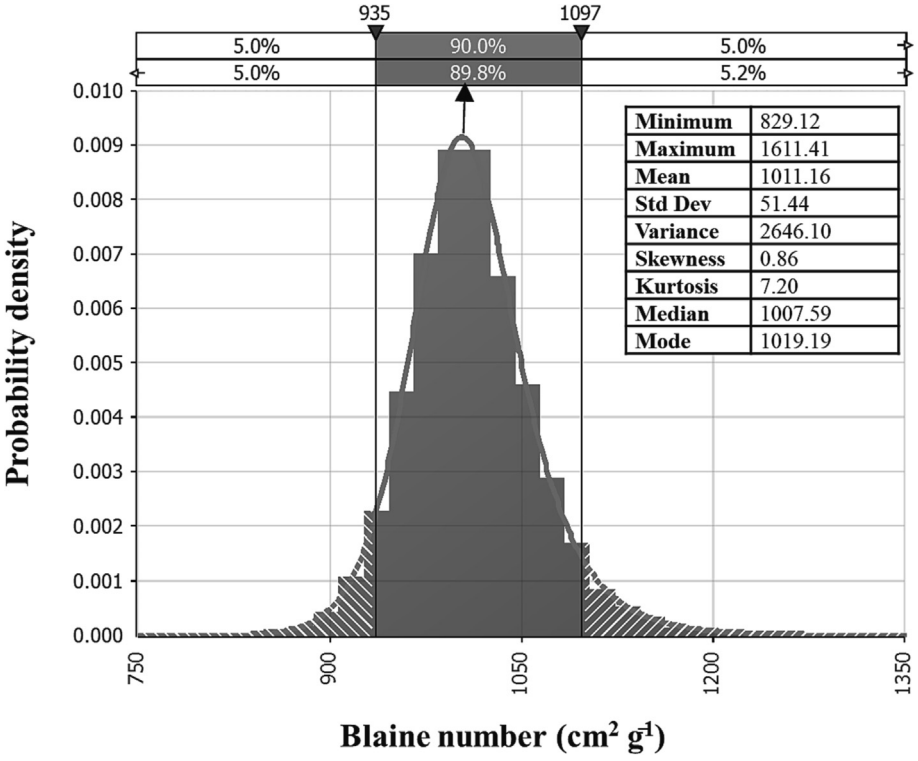

Fig. 10. The histogram and statistical results of simulation for the Blaine number of iron ore concentrates.

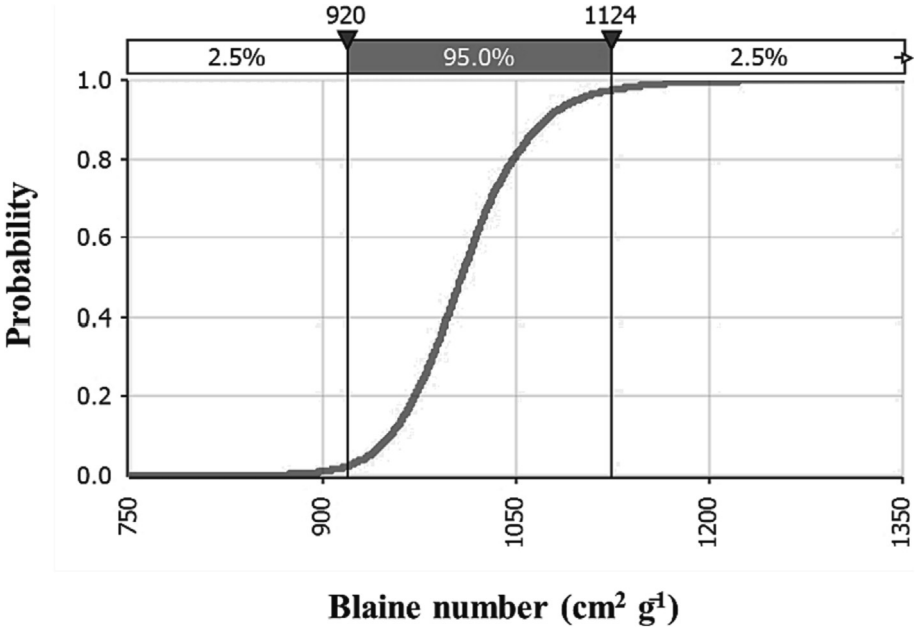

Fig. 11. The cumulative distribution function for the Blaine number of iron ore concentrates.

Blaine number between 1059 $cm^2\ g^{-1}$ and 1097 $cm^2\ g^{-1}$ is 10 %. In other words, the uncertainty of the achieving a Blaine number more than 1097 $cm^2\ g^{-1}$ is 5 %.

4. Conclusions

One of the most important parameters for controlling the pelletizing process in the iron and steel chain is the Blaine number or the specific surface area of iron ore concentrate. The conventional methods of measuring the Blaine number of iron ore concentrate have important challenges such as a long time required from sample preparation to Blaine test, human and systematic errors, high consumption of expensive CRM for daily calibration of the Blaine meter, and the Blaine meter sensitivity to the environmental conditions. To solve the mentioned challenges and limitations, a comprehensive strategy was proposed based on the particle size distribution and shape (controlling the Blaine number) by

combination of Response surface methodology and Monte Carlo simulation. After implementing the proposed strategy for the concentrate obtained from the iron ore processing plant of Gohar Zamin Iron Ore Company, the obtained model was validated by using 228 industrial data from Gohar Zamin Iron Ore Company, Gol-e-Gohar Mining & Industrial Company, and Chadormalu Mining and Industrial Company. The R-square for the proposed model (i.e., 0.9793) was of priority in relation to the quadratic model (i.e., 0.3297). The results showed that in the low values of the B_1 as the representative of the Blaine number of particles + 500 μm (0.10 $cm^2\ g^{-1}$), increasing the B_4 (the representative of the Blaine number of particles + 180–250 μm) from 0.25 $cm^2\ g^{-1}$ to 0.55 $cm^2\ g^{-1}$ result in a significant increase in Blaine number from about 1012 $cm^2\ g^{-1}$ to 1101 $cm^2\ g^{-1}$. Moreover, in the high values of the B_1 (0.30 $cm^2\ g^{-1}$), increasing the B_4 would result in a significant decrease in Blaine number from about 1128 $cm^2\ g^{-1}$ to 970 $cm^2\ g^{-1}$. Finally, the proposed model under uncertainty was analyzed using Monte Carlo simulation. The results showed that the probability of different tests leading to the values of Blaine number between 1059 $cm^2\ g^{-1}$ and 1097 $cm^2\ g^{-1}$ is 10 %. In other words, the uncertainty of the achieving a Blaine number more than 1097 $cm^2\ g^{-1}$ was 5 %. According to the obtained results, the proposed strategy and obtained model can be used as a powerful and relatively accurate technique for modelling and predicting the Baline number of iron ore concentrate produced in industrial plants and a suitable alternative to the conventional measurement methods.

CRediT authorship contribution statement

Seyed Hadi Shahcheraghi: Conceptualization, Investigation, Methodology, Project administration, Software, Writing - original draft, Writing - review & editing.

Declaration of Competing Interest

The authors declare that they have no known competing financial interests or personal relationships that could have appeared to influence the work reported in this paper.

Acknowledgments

This research was supported by Gohar Zamin Iron Ore Company, especially Managing Director (i.e., Dr. Mohammad Mahyapour), Deputy of Operation (i.e., Mr. Amin Fathi), and the Laboratory and Quality Control Unit, which is gratefully acknowledged.

Funding

This work was supported by Gohar Zamin Iron Ore Company [grant number 10860541940].

References

[1] J. Pal, S. Ghorai, T. Venugopalan, Effect of high Blaine iron ore fines in hematite ore pelletization for blast furnace, Miner. Process. Extr, Metall. 129 (2020) 299–307, https://doi.org/10.1080/25726641.2018.1505208.
[2] D.K. Gorai, S. Saida, K.D. Mehta, B.K. Singh, Effect of Blaine Number on the Physical and Mechanical Properties of Iron Ore Pellets, J. Inst. Eng. (india) D (2022) 1–11, https://doi.org/10.1007/s40033-022-00374-6.
[3] S.N. Sahu, P.K. Baskey, S.D. Barma, S. Sahoo, B. Meikap, S.K. Biswal, Pelletization of synthesized magnetite concentrate obtained by magnetization roasting of Indian low-grade BHQ iron ore, Powder Technol. 374 (2020) 190–200, https://doi.org/10.1016/j.powtec.2020.07.004.
[4] K. Barik, P. Prusti, S. Soren, B. Meikap, S. Biswal, Analysis of iron ore pellets properties concerning raw material mineralogy for effective utilization of mining waste, Powder Technol. 400 (2022), https://doi.org/10.1016/j.powtec.2022.117259 117259.
[5] D. Safonov, T. Kinnarinen, A. Häkkinen, An assessment of Blaine's air permeability method to predict the filtration properties of iron ore concentrates, Miner. Eng. 160 (2021), https://doi.org/10.1016/j.mineng.2020.106690 106690.
[6] Y. Ghasemi, M. Emborg, A. Cwirzen, Estimation of specific surface area of particles based on size distribution curve, Mag. Concr. Res. 70 (2018) 533–540, https://doi.org/10.1680/jmacr.17.00045.
[7] B.A. Wills, J. Finch, Wills' mineral processing technology: an introduction to the practical aspects of ore treatment and mineral recovery, Butterworth-Heinemann, 2015.
[8] J. Pal, S. Ghorai, S. Agarwal, B. Nandi, T. Chakraborty, G. Das, S. Prakash, Effect of blaine fineness on the quality of hematite iron ore pellets for blast furnace, Miner. Process. Extr. Metall. Rev. 36 (2015) 83–91, https://doi.org/10.1080/08827508.2013.873862.
[9] R.R. Rhinehart, Nonlinear regression modeling for engineering applications: modeling, model validation, and enabling design of experiments, John Wiley & Sons, 2016.
[10] A. Abazarpoor, M. Halali, R. Hejazi, M. Saghaeian, V.S. Zadeh, Investigation of iron ore particle size and shape on green pellet quality, Can. Metall. Q. 59 (2020) 242–250, https://doi.org/10.1080/00084433.2020.1730116.
[11] F.P. Van Der Meer, Pellet feed grinding by HPGR, Miner. Eng. 73 (2015) 21–30, https://doi.org/10.1016/j.mineng.2014.12.018.
[12] R. Prasad, R. Venugopal, L. Kumaraswamidhas, C. Pandey, S. Pan, Analysis of the Influence of Blaine Numbers and Firing Temperature on Iron Ore Pellets Properties Using RSM-I-Optimal Design: An Approach Toward Suitability, Min. Metall. Explor. 37 (2020) 1703–1716, https://doi.org/10.1007/s42461-020-00282-x.
[13] A. Abazarpoor, M. Halali, R. Hejazi, M. Saghaeian, HPGR effect on the particle size and shape of iron ore pellet feed using response surface methodology, Miner. Process. Extr, Metall. 127 (2018) 40–48, https://doi.org/10.1080/03719553.2017.1284414.
[14] M. Hosseini-Nasab, M.H. Sadeghi, Effect of Particle Size Distribution and Type of Mineral on the Blaine Number, Int. J. Min. Geo-Eng. 54 (2020) 51–57. https://doi.org/10.22059/ijmge.2019.260347.594747.
[15] Y. Zhang, T. Napier-Munn, Effects of particle size distribution, surface area and chemical composition on Portland cement strength, Powder Technol. 83 (1995) 245–252, https://doi.org/10.1016/0032-5910(94)02964-P.
[16] Iso-21283,, Iron ores — Determination of specific surface area — Test method using airpermeability apparatus (Blaine), The International Organization for Standardization (2018).
[17] Astm-c204-16,, Standard Test Methods for Fineness of Hydraulic Cement by Air-Permeability Apparatus, ASTM International, 2017.
[18] I. Odler, The BET-specific surface area of hydrated Portland cement and related materials, Cem. Concr. Res. 33 (2003) 2049–2056, https://doi.org/10.1016/S0008-8846(03)00225-4.
[19] K. Kuhlmann, Correlation of cement particle size and surface area, Zem 37 (1984) 257–259.
[20] M. Sumner, N. Hepher, G. Moir, The influence of a narrow cement particle size distribution on cement paste and concrete water demand, Ciments, bétons, plâtres, chaux, (1989) 164-168.
[21] H. Binici, O. Aksogan, I.H. Cagatay, M. Tokyay, E. Emsen, The effect of particle size distribution on the properties of blended cements incorporating GGBFS and natural pozzolan (NP), Powder Technol. 177 (2007) 140–147, https://doi.org/10.1016/j.powtec.2007.03.033.
[22] ISO-3082, Iron ores — Sampling and sample preparation procedures, 2017.
[23] D.S. Rao, Textbook of Mineral Processing, Scientific Publishers, 2017.
[24] Y. Waseda, A. Muramatsu, Morphology control of materials and nanoparticles: advanced materials processing and characterization, Springer Science & Business Media, 2003.
[25] J. Seville, U. Tüzün, R. Clift, Processing of particulate solids, Springer Science & Business Media, 2012.
[26] K. Higashitani, H. Makino, S. Matsusaka, Powder technology handbook, CRC Press, 2019.
[27] AccuPycII-1345-OperatorManual, GAS DISPLACEMENT PYCNOMETER, 2019.
[28] B. Jones, D.C. Montgomery, Design of Experiments: A Modern Approach, Wiley, 2020.
[29] D.C. Montgomery, Design and Analysis of Experiments, John Wiley & Sons, Limited, 2019.
[30] R.H. Myers, D.C. Montgomery, C.M. Anderson-Cook, Response Surface Methodology: Process and Product Optimization Using Designed Experiments, Wiley, 2016.
[31] G.E. Box, N.R. Draper, Response surfaces, mixtures, and ridge analyses, John Wiley & Sons, 2007.
[32] R.V. Rao, Advanced modeling and optimization of manufacturing processes: international research and development, Springer, 2011.
[33] R. Mukerjee, C.-F. Wu, A modern theory of factorial design, Springer, 2006.
[34] M.J. Anderson, P.J. Whitcomb, RSM simplified: optimizing processes using response surface methods for design of experiments, Productivity Press (2016).
[35] R. Mead, S.G. Gilmour, A. Mead, Statistical principles for the design of experiments: applications to real experiments, Cambridge University Press, 2012.
[36] K. Rekab, M. Shaikh, Statistical design of experiments with engineering applications, Taylor & Francis Boca Raton, FL, 2005.
[37] C. Hirotsu, Advanced analysis of variance, John Wiley & Sons, 2017.

[38] L.S. Meyers, G. Gamst, A.J. Guarino, Applied multivariate research: Design and interpretation, Sage publications, 2016.
[39] S. Mahdevari, M. Hayati, Finite-difference based response surface methodology to optimize tailgate support systems in longwall coal mining, Sci. Rep. 11 (2021) 1–22, https://doi.org/10.1038/s41598-021-82104-8.
[40] B.D. Shaw, Uncertainty analysis of experimental data with R, Chapman and Hall/CRC, 2017.
[41] H.W. Coleman, W.G. Steele, Experimentation, validation, and uncertainty analysis for engineers, John Wiley & Sons, 2018.
[42] S.S. Bahga, Experimental Uncertainty Analysis: A Textbook for Science and Engineering Students, Supreet Singh Bahga (2021).
[43] E. De Rocquigny, Modelling under risk and uncertainty: an introduction to statistical, phenomenological and computational methods, John Wiley & Sons, 2012.
[44] P. Samui, D.T. Bui, S. Chakraborty, R.C. Deo, Handbook of probabilistic models, Butterworth-Heinemann, 2019.
[45] R. Willink, Measurement uncertainty and probability, Cambridge University Press, 2013.
[46] H. Pham, S. Series, Reliab. Eng. (2013).
[47] B. Wu, Reliability analysis of dynamic systems: efficient probabilistic methods and aerospace applications, Academic Press, 2013.
[48] W.K.V. Chan, Theory and applications of Monte Carlo simulations, BoD–Books on Demand, 2013.
[49] D.-G. Chen, J.D. Chen, Monte-Carlo simulation-based statistical modeling, Springer, 2017.
[50] D. Price, A. Maile, J. Peterson-Droogh, D. Blight, A methodology for uncertainty quantification and sensitivity analysis for responses subject to Monte Carlo uncertainty with application to fuel plate characteristics in the ATRC, Nucl. Eng. Technol. 54 (2022) 790–802, https://doi.org/10.1016/j.net.2021.09.010.
[51] X. Hu, G. Fang, J. Yang, L. Zhao, Y. Ge, Simplified models for uncertainty quantification of extreme events using Monte Carlo technique, Reliab. Eng. Syst. Saf. 230 (2023), https://doi.org/10.1016/j.ress.2022.108935 108935.
[52] G. Xie, A novel Monte Carlo simulation procedure for modelling COVID-19 spread over time, Sci. Rep. 10 (2020) 1–9, https://doi.org/10.1038/s41598-020-70091-1.
[53] M. Hayati, S.M.S.A. Ganji, S.H. Shahcheraghi, R.R. Khabir, Optimization of copper recovery from electronic waste using response surface methodology and Monte Carlo simulation under uncertainty, J. Mater. Cycles Waste Manag. 25 (2023) 211–220, https://doi.org/10.1007/s10163-022-01526-2.
[54] D.P. Kroese, T. Taimre, Z.I. Botev, Handbook of monte carlo methods, John Wiley & Sons, 2013.
[55] G.P. Rangaiah, A. Bonilla-Petriciolet, Multi-objective optimization in chemical engineering: developments and applications, John Wiley & Sons, 2013.
[56] D. Sbárbaro, R., Del Villar, Advanced control and supervision of mineral processing plants, Springer Science & Business Media, 2010.
[57] S.L. Fegade, B.M. Tande, H. Cho, W.S. Seames, I. Sakodynskaya, D.S. Muggli, E.I. Kozliak, Aromatization of propylene over Hzsm-5: A design of experiments (DOE) approach, Chem. Eng. Commun. 200 (2013) 1039–1056, https://doi.org/10.1080/00986445.2012.737385.